Wake-field generation by the ponderomotive memory effect

U. Wolf and H. Schamel
Physikalisches Institut, Universität Bayreuth, D-95440 Bayreuth, Germany
(Received 13 January 1997; revised manuscript received 31 March 1997)

An analytical and numerical investigation of the plasma response to an imposed high frequency wave packet with a slow explicit time-dependent envelope is presented. An underlying picture of ponderomotive effects is developed, which shows that the explicit time dependence forces us to treat the problem kinetically, and furthermore, that a wake field is generated by the ponderomotive memory effect. The latter supplements the well-known ponderomotive force and fake heating effect. Several perturbation schemes are compared showing that the influence of resonant particles, treated by the method of characteristics, has to be taken into account for Langmuir wave packets with $k\lambda_d \geqslant 0.2$, where k is the wave number and λ_d the Debye length. A self-consistent Vlasov simulation shows the disappearance of the density depression in the case of immobile ions, whereas the wake-field pattern survives self-consistency. [S1063-651X(97)05010-1]

PACS number(s): 52.25.−b, 52.35.Mw, 52.40.Nk

I. INTRODUCTION

The concept of wake-field acceleration of charged particles in plasmas relies on the idea that some external agent, such as a laser or an electron beam, induces an internal plasma oscillation in which test particles are accelerated [1–15]. This way one hopes to overcome the limitations of conventional particle accelerators which are limited in the obtainable acceleration gradients by the breakdown of electric fields through ionization. A plasma is already an ionized material, and can stand electric fields which would otherwise destroy the materials used in conventional accelerators. In the laser wake-field acceleration scheme, a laser pulse traveling through the plasma induces an electric wake field by the ponderomotive force accelerating charged particles.

In the present paper, we explore the generation of wake fields caused by an explicit time dependence of the high frequency wave envelope which, for simplicity, is chosen to be an electrostatic Langmuir wave packet. We show that, besides the ponderomotive force, there is an additional ponderomotive effect, the so-called ponderomotive memory effect, which is caused by an explicit time dependence of the ponderomotive potential $|E|^2$, where E is the wave envelope. Whereas the former is given by the gradient of $|E|^2$, $\partial_x|E|^2$, the latter results mathematically from an integration of $\partial_t|E|^2$ along the unperturbed characteristics, and is hence purely kinetic ([16,17]). Indications that such a process can work in reality are provided by experiments [18], where bunches of accelerated ions with velocities up to $7c_s$ were detected, c_s being the ion acoustic velocity. In these experiments, a high-field intensity localized in space and time was generated in the peak of a converging cone by microwave emission from a ring antenna [18]. Since T_i/T_e is in the 0.04–0.2 range, a thermal ion with $v_{\mathrm{thi}} \equiv 0.2-0.4c_s$ typically experienced an increase of its velocity by a factor of 20.

In the present paper, we pay attention to the first part of this acceleration process, the production of wake fields. This paper is organized as follows. In Sec. II we present the passive response of electrons on the slow time scale under the assumption that resonant particle effects are negligible or weak, and develop the underlying picture of ponderomotive effects. We shall see that, even if the perturbation is weak ($|E|^2 \ll 1$) and the unperturbed plasma is assumed to be thermal, the explicit time dependence of E places the problem in the kinetic regime. That is, $\partial_t|E|^2$ acts as a source and excites almost spontaneously an infinite number of hydrodynamic moments for short pulses. The main effect of $\partial_t|E|^2$, the generation of wakes (or ponderomotive streamers), can therefore not be studied in a macroscopic description of ponderomotive effects.

In Sec. III resonant particle effects are fully taken into account, and comparisons are made with the results obtained in Sec. II. In Sec. IV a Vlasov simulation is applied to check the validity and limits of the theoretical analysis. In Sec. V, these results are summarized.

II. ANALYTICAL TREATMENT OF THE PASSIVE PROBLEM WITH THE NEUMANN SERIES

We study a plasma on the electronic time scale, assuming that the ions are immobile and constitute a neutral background. First, we ignore self-consistency. An external electrostatic hf wave having a weak time- and space-dependent envelope is applied to the plasma. Therefore, we can use the Ansatz $E_{\mathrm{tot}}(x,t) \sim E^*(x-v_g t,t)\exp[i(kx-\omega t)]$, E being the amplitude of the electric field and v_g the group velocity of the wave packet. First we assume that the group velocity is small, so that we are allowed to neglect it in the amplitude of the electric field, i.e., we set $k=0=v_g$ and use a normalized carrier frequency $\omega=1$.

A. Calculation of the distribution function neglecting the group velocity

We describe the plasma by the Vlasov equation

$$\left\{ L - [E(x,t)e^{it} + E^*(x,t)e^{-it}] \frac{\partial}{\partial v} \right\} f(x,v,t) = 0, \quad (1)$$

where L is the unperturbed (free-streaming) Vlasov operator

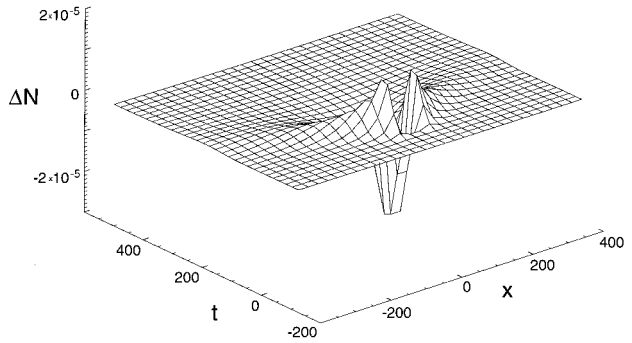

FIG. 1. The density perturbation as a function of space and time, as obtained by the Neumann series. Here $\epsilon=0.157$, $\sigma_x=10.0$, $\sigma_t=25.0$, and $k=0.0$.

$$L:=\frac{\partial}{\partial t}+v\frac{\partial}{\partial x}, \tag{2}$$

and where we make the following assumptions. (1) When the electric field vanishes, the plasma is in a thermal equilibrium state having the Maxwell distribution function $f_M(v)$: $=(1/\sqrt{2\pi})e^{-(v^2/2)}$; in this sense the amplitude of the electric field constitutes a smallness parameter. (2) There is only a negligible amount of resonant particles, and the distribution function obeys the inequality $|Lf(x,v,t)|\ll|f(x,v,t)|$. (3) We consider Langmuir waves with a negligible wave number. Because of the small time dependence of the electric wave amplitude we can make the *Ansatz* [19]

$$f(x,v,t)=\overline{f}(x,v,t)+\sum_{n=1}^{\infty}[F_n(x,v,t)e^{int}+\text{c.c.}], \tag{3}$$

$\overline{f}$ being the slowly varying part of the distribution function which we want to calculate. For the first two Fourier modes we obtain the equations

$$L\overline{f}=E\frac{\partial F_1^*}{\partial v}+E^*\frac{\partial F_1}{\partial v} \tag{4}$$

and

$$(i+L)F_1=E\frac{\partial\overline{f}}{\partial v}+E^*\frac{\partial F_2}{\partial v}. \tag{5}$$

Introducing the smallness parameter $\epsilon=O(E)$, we make use of assumption (1) and expand the Fourier modes in a series:

$$\overline{f}=f_M+\sum_{m=1}^{\infty}\epsilon^m f^{(m)} \quad\text{and}\quad F_n=\sum_{m=1}^{\infty}\epsilon^m F_n^{(m)}. \tag{6}$$

The first-order equation for the slowly varying distribution reads $Lf^{(1)}=0$. Since we assume a Maxwellian plasma in the absence of an electric field, we put $f^{(1)}\equiv 0$. For that reason, the long time-scale distribution function is given by $\overline{f}=f_M+\epsilon^2 f^{(2)}+O(\epsilon^3)$. Therefore, we have to calculate $f^{(2)}$. The second-order perturbation is given by the equation

$$Lf^{(2)}=E\frac{\partial F_1^{(1)^*}}{\partial v}+E^*\frac{\partial F_1^{(1)}}{\partial v}. \tag{7}$$

We recognize that the first Fourier mode of the first-order perturbation is driven by the electric field

$$(i+L)F_1^{(1)}=E\frac{df_M}{dv}. \tag{8}$$

Assumption (2) guarantees the existence of the operator $[1+(L/i)]^{-1}$, and its expression by a geometric series to solve Eq. (8) for $F_1^{(1)}$:

$$F_1^{(1)}=\sum_{n=0}^{\infty}\left(\frac{L}{-i}\right)^n\left(E\frac{\frac{df_M}{dv}}{i}\right). \tag{9}$$

Therefore, in $O(\epsilon^2)$ the following differential equation is found:

$$L\overline{f}=\partial_v(E^*LE+\text{c.c.})\partial_v\overline{f}. \tag{10}$$

This is a diffusion equation in phase space with a slowly varying space- and time-dependent diffusion coefficient [16]. Integrating along the characteristics of the unperturbed problem we obtain the solution for $\overline{f}$:

$$\begin{aligned}\overline{f}&=\frac{\exp\left[-\frac{v^2}{2(1+2\psi)}-\psi\right]}{\sqrt{2\pi(1+2\psi)}}(1+M)\\&\approx f_M[1+(v^2-2)\psi+M],\end{aligned} \tag{11}$$

where M is defined by

$$M=\int_{-\infty}^{t}\frac{\partial\psi}{\partial\tilde{t}}(\tilde{x},\tilde{t})\Big|_{\substack{\tilde{x}=x+v(\tau-t)\\ \tilde{t}=\tau}}\quad d=\tau. \tag{12}$$

Here $\psi:=|E|^2$ is the ponderomotive potential appearing in the exponential and giving rise to a density depression $n=e^{-\psi}\approx 1-\psi$. ψ also appears in the denominator of the argument of the exponential in Eq. (11), and in the normalization factor. It represents an increase of the effective temperature by 2ψ called ''fake heating'' [20]. The third term M is an integral where the time derivative of ψ is summed up along the characteristics at earlier times, $\tau<t$. Hence, this term represents a memory of the system [16,21].

Defining the macroscopic quantities as usual, from Eq. (11) we obtain the density n, the mean velocity u, the pressure p, and the heat flux w:

$$\begin{aligned}n(x,t)&=1-\psi(x,t)+A_0(x,t),\\u(x,t)&=A_1(x,t),\\p(x,t)&=1+\psi(x,t)+A_2(x,t),\\w(x,t)&=-3A_1(x,t)+A_3(x,t),\end{aligned} \tag{13}$$

where the quantity A_l is given by

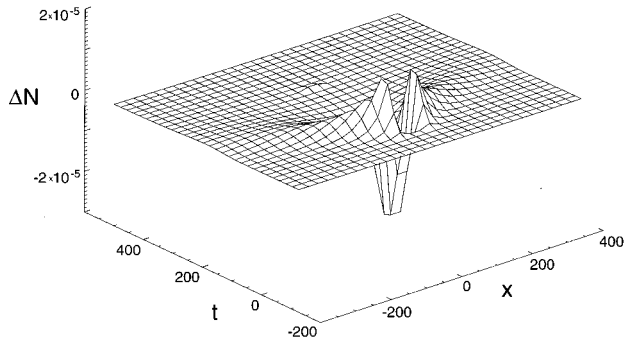

FIG. 2. The density perturbation as a function of space and time, as obtained by the characteristic method. Here $\epsilon=0.157$, $\sigma_x=10.0$, $\sigma_t=25.0$, and $k=0.0$.

$$A_l(x,t)=\frac{1}{\sqrt{2\pi}}\int_{-\infty}^{\infty}\exp\left(-\frac{v^2}{2}\right)v^l M(x,v,t)\,dv. \quad (14)$$

It can easily be verified that

$$\frac{\partial A_l}{\partial t}(x,t)+\frac{\partial A_{l+1}}{\partial x}(x,t)=R_l\frac{\partial \psi}{\partial t}(x,t) \quad (15)$$

holds.

Here

$$R_l\equiv\frac{1}{\sqrt{2\pi}}\int_{-\infty}^{\infty}\exp\left(-\frac{v^2}{2}\right)v^l dv=\begin{cases}0: & l \text{ odd}\\ (l-1)!!: & l \text{ even.}\end{cases} \quad (16)$$

From Eq. (15), it follows that A_{l+1} plays the role of a current density with respect to the density A_l, and that this new type of moment is generated by the source term $\partial_t\psi$. Note that the generation of odd moments, such as the mean velocity and the heat flux, is entirely due to the action of the ponderomotive memory effect [17]. Equation (15) shows that a temporal pulselike envelope excites rather instantaneously an infinite number of velocity moments; the generation is more effective for the higher degrees momenta. Hence, even if the unperturbed plasma is Maxwellian, a time-dependent (macroscopic) electric field applied to a collisionless plasma, casts the physics immediately into the kinetic regime. There is, therefore, no chance of a hydrodynamic closure, i.e., of a representation of the system by a finite number of hydrodynamic equations. Figure 1, where $\Delta N\equiv n-1$ is plotted as a function of space and time for a Gaussian-shaped ponderomotive potential [see Eq. (27)], exhibits both the formation of a density depression, represented by $-\psi$, and the generation of a wake field, represented by A_0. The latter emanates from the origin, $x=0$, $t=0$, the location in space-time, where ψ is maximum.

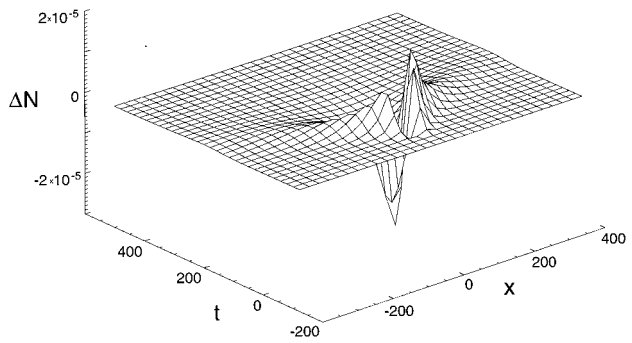

FIG. 3. Same as Fig. 1, except that $k=0.1$.

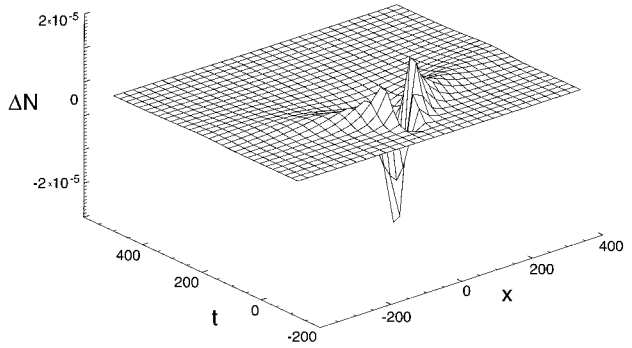

FIG. 4. Same as Fig. 2, except that $k=0.1$.

B. Calculation of the distribution function in the case of finite group velocity

Next we extend our theory by considering finite k and a finite group velocity in the envelope of the wave. Moreover, we consider the effect of a time-independent ambipolar potential which may arise due to charge separation. Again we start with the Vlasov equation (for clarity, we retain the symbol ω):

$$\left\{L-[E(x-v_g t,t)e^{-i(kx-\omega t)}+\text{c.c.}]\,\frac{\partial}{\partial v}\right\}f(x,v,t)=0,$$

where the operator

$$L:=\frac{\partial}{\partial t}+v\frac{\partial}{\partial x}-\Phi'(x)\,\frac{\partial}{\partial v}. \quad (17)$$

Here $-\Phi'$ is the time-independent, ambipolar electrostatic field. We make the following assumptions. (1) The distribution of the electrons without an electric field is described by a solution of the free Vlasov operator, $Lf_0=0$. Therefore, f_0

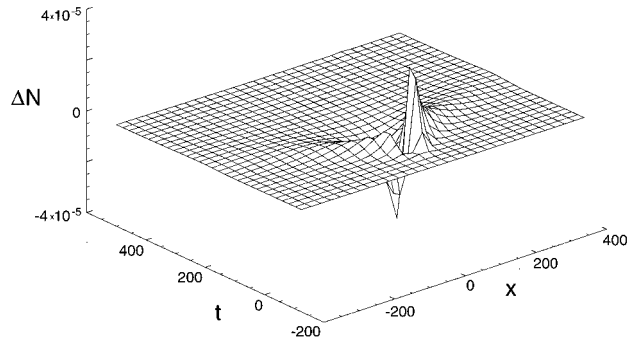

FIG. 5. Same as Fig. 1, except that $k=0.2$.

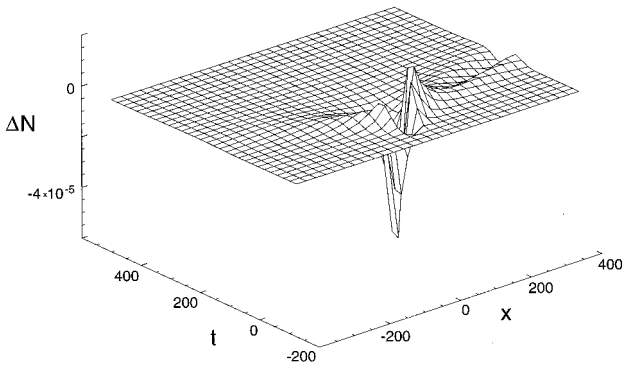

FIG. 6. Same as Fig. 2, except that $k=0.2$.

can be any function of the constants of motion. We choose $f_0(x,v)=(1/\sqrt{2\pi})\exp[-(v^2/2)+\Phi(x)]$. (2) The slowly varying amplitude of the electric field is small. (3) There are only a few resonant particles. (4) The wave vector is small. With the Ansätze (3) and (6), we again get the distribution function $\overline{f}=f_0+\epsilon^2 f^{(2)}+O(\epsilon^3)$. Therefore, we have to solve the system

$$Lf^{(2)}=E^{\star}(x-v_g t,t)\,\frac{\partial F_1^{(1)}}{\partial v}+E(x-v_g t,t)\,\frac{\partial F_1^{(1)\star}}{\partial v} \tag{18a}$$

and

$$[-i(kv-\omega)+L]F_1^{(1)}=E(x-v_g t,t)\frac{\partial f_0}{\partial v}\,. \tag{18b}$$

As in the previous section, assumption (3) permits us to use the Neuman series

$$F_1^{(1)}(x,v,t)=\sum_{-n=0}^{\infty}[L/i(kv-\omega)]^n \times\left[\frac{E(x-v_g t,t)\,\dfrac{\partial f_0}{\partial v}(x,v)}{-i(kv-\omega)}\right].$$

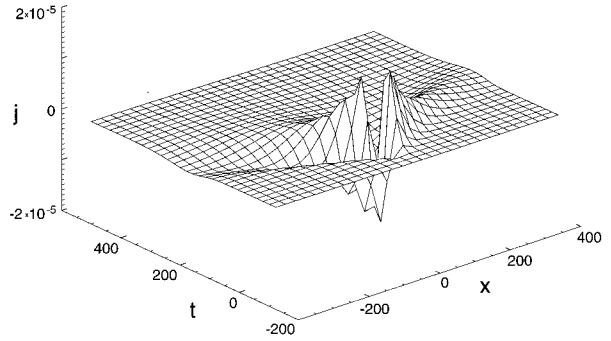

FIG. 7. The current density as a function of space and time, as obtained by the Neumann series. Here $\epsilon=0.157$, $\sigma_x=10.0$, $\sigma_t=25.0$, and $k=0.0$.

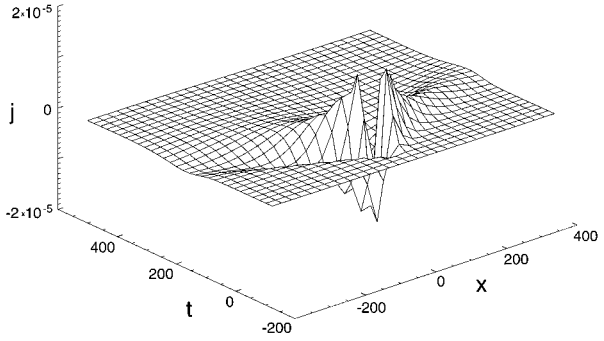

FIG. 8. The current density as a function of space and time, as obtained by the characteristic method. Here $\epsilon=0.157$, $\sigma_x=10.0$, $\sigma_t=25.0$, and $k=0.0$.

Truncating at the second order and setting $F_1^{(1)}$ into Eq. (18a), we end up with the following kinetic equation for the slowly varying distribution function:

$$\begin{aligned}L\overline{f}=&\frac{1}{(kv-\omega)^2}\frac{\partial\overline{f}}{\partial v}\frac{\partial\psi}{\partial x}(x-v_g t,t)+\frac{\partial}{\partial v}\left[\frac{\partial\overline{f}}{\partial v}\frac{1}{(kv-\omega)^2}\right]\\&\times L\psi(x-v_g t,t)-2\psi(x-v_g t,t)\,\frac{\partial}{\partial v}\left[\frac{\dfrac{\partial\overline{f}}{\partial x}}{(kv-\omega)^2}\right]\\&+2\psi\frac{\partial}{\partial v}\left[\frac{\dfrac{\partial\overline{f}}{\partial v}}{kv-\omega}\Phi'\frac{\partial}{\partial v}\left(\frac{1}{kv-\omega}\right)\right],\end{aligned} \tag{19}$$

where again $\psi:=|E|^2$. In the case $k\to 0,\omega\to 1$ and neglecting the time dependence of the electric-field amplitude, we recover the kinetic equation of Aamodt and Vella [20].

Next, we look at the hydrodynamic equations resulting from the new kinetic equation:

$$\frac{\partial n}{\partial t}+\frac{\partial}{\partial x}(nu)=0 \tag{20}$$

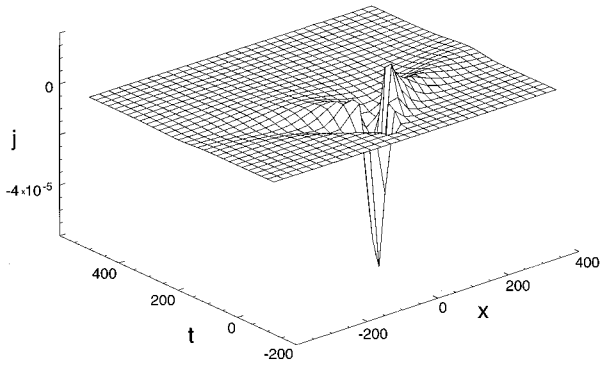

FIG. 9. Same as Fig. 7, except that $k=0.2$.

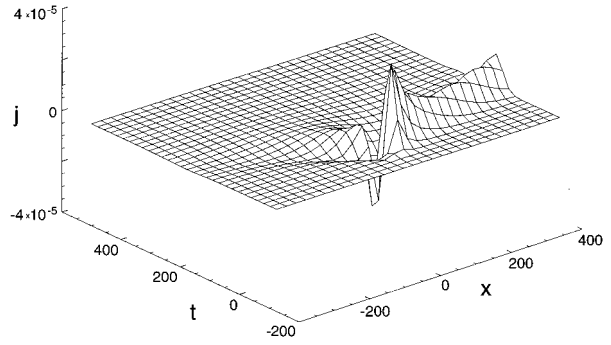

FIG. 10. Same as Fig. 8, except that $k=0.2$.

and

$$\frac{\partial u}{\partial t}+u\frac{\partial u}{\partial x}=\Phi'-\frac{1}{\omega^2}\frac{\partial \psi}{\partial x}(x-v_g t,t)-\frac{1}{n}\frac{\partial}{\partial x}\Big[p-\frac{2n}{\omega^2}\times\psi(x-v_g t,t)\Big]+\frac{2k}{\omega^3}\Big\{\frac{\partial\psi}{\partial t}(x-v_g t,t)+\frac{2}{n}\frac{\partial}{\partial x}[un\psi(x-v_g t,t)]\Big\}-\frac{6k^2}{\omega^4}\psi(x-v_g t,t)\Phi', \tag{21}$$

where n, u, and p denote the particle density, particle velocity, and pressure moment, respectively. Φ' is the force arising from the ambipolar electric field. As a second force we recognize the well-known ponderomotive force $(1/\omega^2)(\partial\psi/\partial x)$. The third part of the sum is the pressure. We recognize that the pressure acting on a fluid element is reduced by the radiation pressure. A similar pressure reduction can be found in the energy law [17]. In fact Eqs. (20) and (21) reduce to Eqs. (22a) and (22b) of that paper in the limit $k\to 0$, $v_g\to 0$.

III. ANALYTICAL TREATMENT OF THE PASSIVE PROBLEM USING CHARACTERISTICS

In Sec. II we computed the first-order distribution function by using the Neumann series [Eqs. (5) and (18)]. This treatment was justified by assuming that the effect of the resonant particles can be neglected. Since we allowed for a finite wave vector k, there are particles for which the resonance $\omega-kv=0$ is satisfied. For these resonant particles, the Neumann series clearly diverges. It can be questioned whether the distribution function is still correctly computed. Therefore, in this section we compute the distribution function directly by using the method of characteristics instead of the Neumann series and compare both results. Again, we start with the Vlasov equation (17) and neglect $\Phi(x)$. Using the same procedure as in Sec. II, we arrive at the system

$$Lf^{(2)}=E^*(x-v_g t,t)\frac{\partial F_1^{(1)}}{\partial v}+E(x-v_g t,t)\frac{\partial F_1^{(1)^*}}{\partial v}(x,v,t) \tag{22}$$

and

$$[-i(kv-\omega)+L]F_1^{(1)}=E(x-v_g t,t)\frac{df_M}{dv}(v). \tag{23}$$

We solve Eq. (23) by integrating along the characteristics of the unperturbed system:

$$F_1^{(1)}(x,v,t)=\int_{-\infty}^{t}\exp[-i(kv-\omega)\times(\tau-t)]E(\hat{x}(\tau),\tau)d\tau\frac{df_M(v)}{dv},$$

where

$$\hat{x}(\tau)=x-vt+(v-v_g)\tau. \tag{24}$$

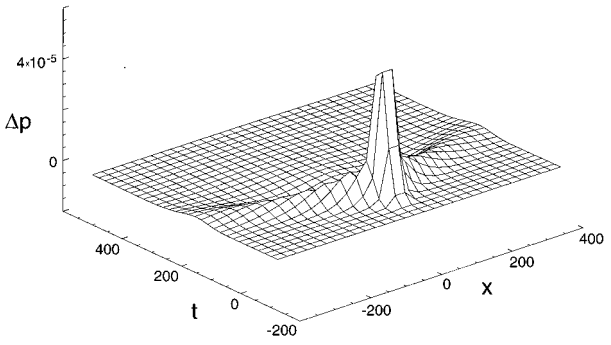

FIG. 11. The pressure perturbation as a function of space and time, as obtained by the Neumann series. Here $\epsilon=0.157$, $\sigma_x=10.0$, $\sigma_t=25.0$, and $k=0.0$.

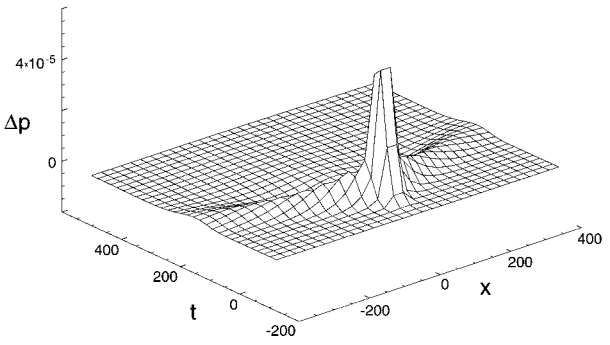

FIG. 12. The pressure perturbation as a function of space and time, as obtained by the characteristic method. Here $\epsilon=0.157$, $\sigma_x=10.0$, $\sigma_t=25.0$, and $k=0.0$.

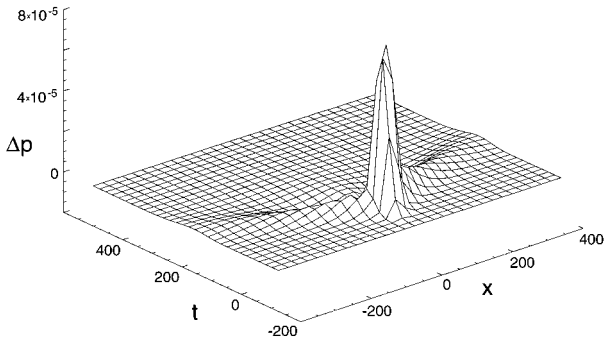

FIG. 13. Same as Fig. 11, except that $k=0.1$.

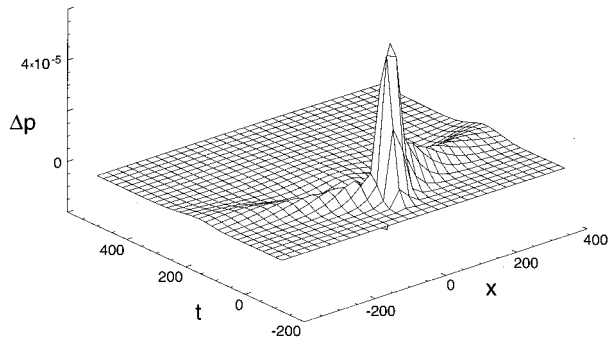

FIG. 14. Same as Fig. 12, except that $k=0.1$.

We set this result into Eq. (22). Then we must solve

$$Lf^{(2)}(x,v,t)=E(x-v_g t,t)\frac{\partial}{\partial v}\left[\int_{-\infty}^{t} e^{i(kv-\omega)(\tau-t)} \times E^*(x-vt+(v-v_g)\tau,\tau)\frac{df_M}{dv}(v)\right]+\text{c.c.} \tag{25}$$

Once more, we integrate along the characteristics and end up with the following result for the second-order perturbation of the distribution function

$$\begin{aligned} f^{(2)}(x,v,t)=2f_M(v)\mathrm{Re}\Bigg\langle &\int_{-\infty}^{0} E(x+v\tau-v_g(\tau+t),\tau+t) \\ &\times\Bigg\{[v^2-1]\int_{-\infty}^{0}[e^{i(kv-\omega)\tau'}E^*(x-vt+(v-v_g) \\ &\times(\tau'+\tau+t),\tau'+\tau+t)]d\tau' \\ &-v\int_{-\infty}^{0}\tau' e^{i(kv-\omega)\tau'}\Bigg[ikE^*(x-vt+(v-v_g) \\ &\times(\tau'+\tau+t),\tau'+\tau+t)+\frac{\partial E^*}{\partial x}(x-vt+(v \\ &-v_g)(\tau'+\tau+t),\tau'+\tau+t)\Bigg]d\tau'\Bigg\}d\tau\Bigg\rangle, \end{aligned} \tag{26}$$

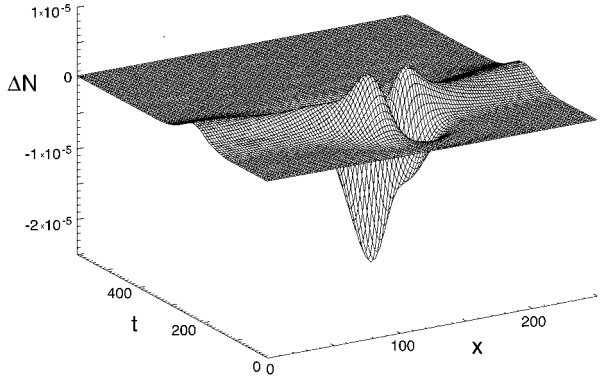

FIG. 15. The density perturbation as a function of space and time obtained using the Vlasov code (parameter set as in Fig. 2).

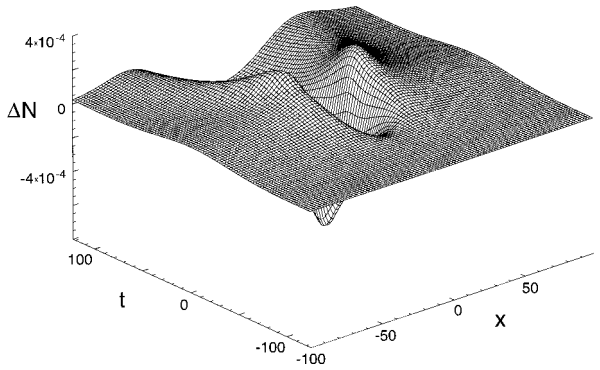

FIG. 16. Same as Fig. 2, except that $\epsilon=1.57$.

where Re denotes the real part. Next we want to compare both methods. With this in mind we introduce the following model for the ponderomotive potential:

$$\psi(x,t)=\frac{\epsilon}{2\pi\sigma_x\sigma_t}\exp[-x^2/2\sigma_x^2-t^2/2\sigma_t^2], \tag{27}$$

where σ_x and σ_t are the mean deviations in x and t, which measure how the potential is centered around the origin in space and time. Now we can calculate $f^{(2)}$, with the result that

$$f^{(2)}(x,v,t)=\frac{\epsilon}{2\pi\sigma_x\sigma_t}f_M(v)\left(\frac{\pi}{p(v)}\right)^{1/2}\{\mathcal{G}_1(v)+\mathcal{G}_2(v)\}. \tag{28}$$

Here, we use the following notation

$$\begin{aligned} \mathcal{G}_1(v)=\mathrm{Re}\Bigg\langle -\frac{i\alpha(v)}{\sqrt{\pi p(v)}}\Bigg\{\beta(v)\Bigg[\frac{1}{2}G(-\sqrt{2}u_0(v),\delta(v)) \\ -i\left(\frac{\pi}{8}\right)^{1/2}\mathrm{erfc}(\sqrt{2}u_0(v))\Bigg]+\frac{1}{\sqrt{2}}[\gamma(v) \\ -\beta(v)\delta(v)i]F(-\sqrt{2}u_0(v),\delta(v))\Bigg\}\Bigg\rangle, \end{aligned} \tag{29a}$$

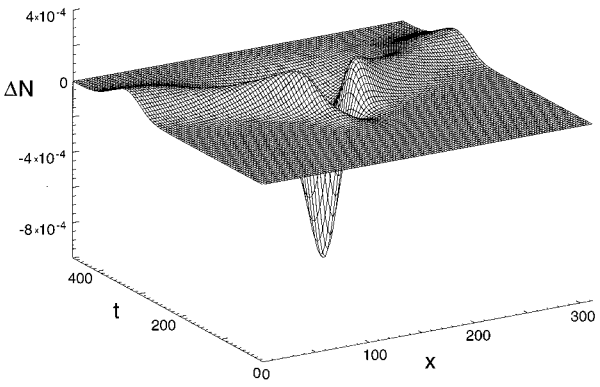

FIG. 17. Same as Fig. 15, except that $\epsilon=1.57$.

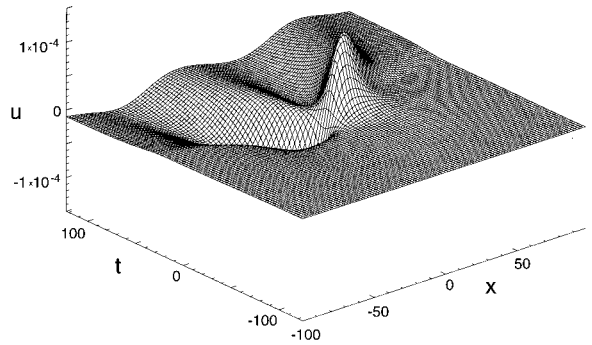

FIG. 18. The fluid velocity as a function of space and time obtained analytically. Here $\epsilon=1.57$, $\sigma_x=10.0$, $\sigma_t=25.0$, and $k=0.0$.

$$\alpha(v)=\exp\left[-\frac{(x-vt)^2}{8\sigma_x^2\sigma_t^2 p(v)}\right], \tag{29b}$$

$$\beta(v)=\frac{v}{8\sigma_x^2\sigma_t^2[p(v)]^{3/2}}\{[2i\sigma_t^2(kv_g-\omega)-t]v+x-2i[k\sigma_x^2+\sigma_t^2 v_g(kv_g-\omega)]\}, \tag{29c}$$

$$\gamma(v)=v^2-1+\frac{v}{4\sigma_x^2 p(v)}\left\{[v-v_g]\left[1-\frac{(kv-\omega)^2}{2p(v)}\right]+2\sigma_x^2(kv-\omega)\left(k+i\,\frac{x-vt}{8\sigma_x^2\sigma_t^2 p(v)}\right)\right\}, \tag{29d}$$

$$\delta(v)=-\frac{kv-\omega}{2\sqrt{p(v)}}, \tag{29e}$$

$$u_0(v)=-\frac{(x-vt)(v-v_g)+4\sigma_x^2 p(v)t}{4\sigma_x^2\sqrt{p(v)}}, \tag{29f}$$

$$p(v)=\frac{\sigma_x^2+(v-v_g)^2\sigma_t^2}{4\sigma_x^2\sigma_t^2}, \tag{29g}$$

$$F(x,y)=\int_{-\infty}^{x} e^{-u^2} Z\left(y-\frac{i}{\sqrt{2}}u\right)du, \tag{29h}$$

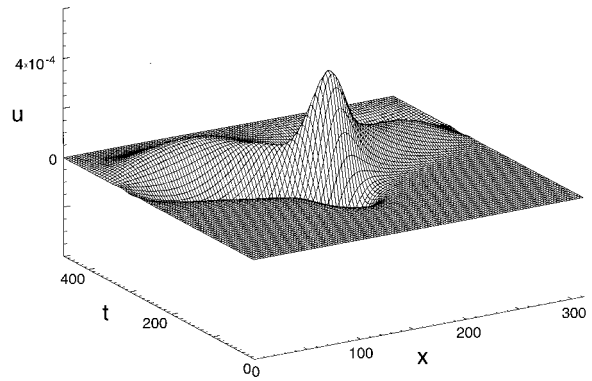

FIG. 19. The fluid velocity as a function of space and time obtained using the Vlasov code (parameter set as in Fig. 18).

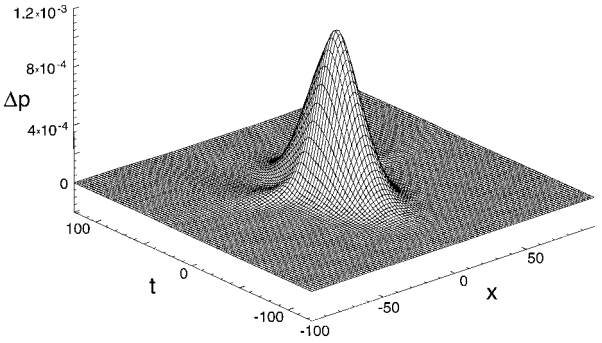

FIG. 20. The pressure perturbation as a function of space and time obtained analytically (parameter set as in Fig. 12, except that $\epsilon=1.57$).

$$G(x,y)=e^{-x^2}Z\left(y-\frac{i}{\sqrt{2}}x\right), \tag{29i}$$

$$Z(\zeta)=2ie^{-\zeta^2}\int_{-\infty}^{i\zeta} e^{-t^2}dt, \tag{29j}$$

and

$$\mathcal{G}_2(v)=-\frac{v(x-vt)}{4\sigma_x^2\sqrt{2}p(v)}\left[1-\frac{(v-v_g)^2}{4\sigma_x^2 p(v)}\right]\times\exp\left\{-\frac{(x-vt)^2}{8\sigma_x^2\sigma_t^2 p(v)}\right\}\times\mathrm{erfc}\left\{-\frac{\sigma_x^2 t+\sigma_t^2(x-v_g t)(v-v_g)}{\sigma_x^2\sigma_t^2\sqrt{8p(v)}}\right\}. \tag{29k}$$

Now, we can compare both methods by calculating the moments of the distribution function. Therefore, we define

$$\mathcal{M}_l(x,t)=R_l+\mathcal{B}_l(x,t), \tag{30a}$$

where R_l is given by Eq. (16), and $\mathcal{B}_l$ by

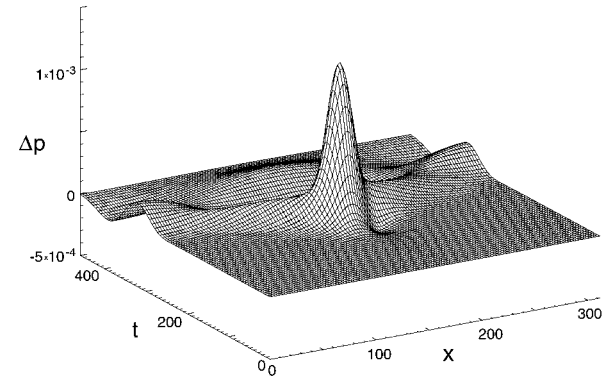

FIG. 21. The pressure perturbation as a function of space and time obtained using the Vlasov code (parameter set as in Fig. 20).

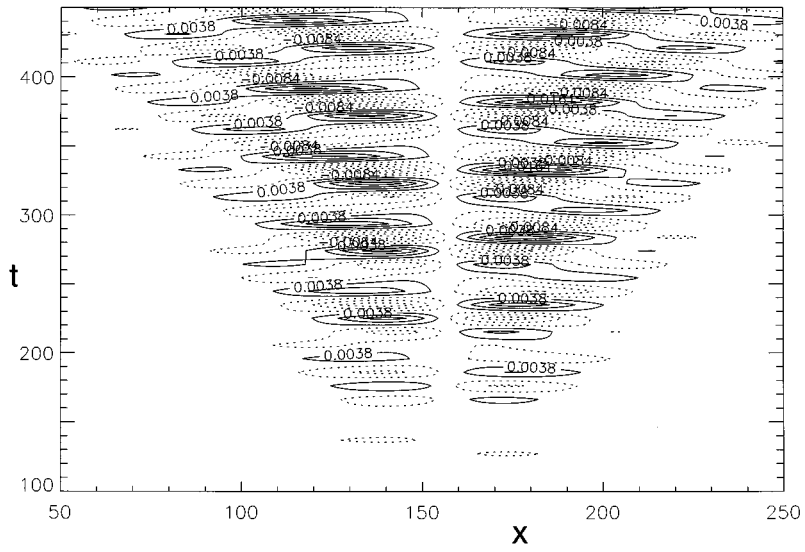

FIG. 22. The unaveraged density perturbation as a function of space and time obtained using the self-consistent Vlasov simulation. Here $\epsilon=0.157$, $\sigma_x=10.0$, and $\sigma_t=50.0$.

$$\mathcal{B}_l(x,t)=\int_{-\infty}^{\infty} v^l f^{(2)}(x,v,t)dv. \tag{30b}$$

$\mathcal{M}_0$ is the particle density, $\mathcal{M}_1$ describes the electron velocity, and $\mathcal{M}_2$ measures the electron temperature. Therefore, $\mathcal{B}_l$ describes the deviation of the moments from their equilibrium value. As we want to investigate whether the Neumann series is describing the first-order distribution well, we have to choose the parameters in the Gauss function correctly to be able to neglect the L^3 term. For that purpose, the following conditions have to be satisfied: $O(\partial_t)\gg O(\partial_x^3)$ and $O(\partial_t)\gg O(|E|^2\partial_x)$. We use $\sigma_x=10$, $\sigma_t=25$, and $\epsilon=0.157$, and find that the field amplitude $|E|^2=10^{-4}$. We also have $1\gg 0.04=(1/\sigma_t)\sim O(\partial_t)\gg 0.001=(1/\sigma_x^3)\sim O(\partial_x^3)$, and $1\ll 25\ll 10^9=\sigma_x/\max\{|E(x,t)|^2:(x,t)\in\mathcal{R}^2\}$. Thus the required inequalities are satisfied. Figure 2 shows the density excursion from its equilibrium value as obtained by the method of characteristics. Since k was chosen to be zero, it should coincide with the Neumann result in Fig. 1, as it indeed does. This validates both our analytical approach, as well as the numerical evaluation of the integrals. Next, we set $k=0.1$. Both methods (see Figs. 3 and 4) yield approximately the same result. However, by increasing the wave number the agreement degrades due to the different treatment of the effect of resonant particles. By comparing both density expressions for $k=0.2$, as given in Figs. 5 and 6, we recognize a difference, especially in the wake-field pattern propagating in the positive x direction. Next we study the current density in the plasma. In the case of $k=0$, the system is homogenous; therefore, the current density is an odd function. Both the Neumann series in Fig. 7 and the method of characteristics in Fig. 8 yield the same result. For a finite wave number $k=0.2$ the phase $\omega-kv$ appears in the denominator, and can be resonant. As the phase velocity of the wave is now closer to the thermal velocity of the plasma, there are enough resonant particles to cause the results from the Neumann method (Fig. 9) to differ from those obtained by an integration along the unperturbed characteristics of the system (Fig. 10). Again, it is the positively propagating wakefield that predominantly changes. Next, we look at the deviation of the pressure from equilibrium ($\Delta p=p-1$). For a standing wave ($k=0$) there is no preferred direction. The pressure moment is an *even* function (Figs. 11 and 12). For $k=0.1$ this symmetry is broken (see Fig. 14). The propagation direction of the applied wave packet defines a preferred direction. Also, the results of the Neumann series (Fig. 13) and of the method of characteristics (Fig. 14) differ from each other because of the resonant particle effect.

IV. VLASOV SIMULATIONS

Here we want to compare our analytical results from Sec. III with a numerical calculation using a Vlasov code. We prescribe periodic boundary conditions in the space variable and homogenous boundary conditions in the velocity variable. To solve the Vlasov equation numerically, we use the splitting scheme of Cheng and Knorr [22]. The Vlasov equation is split up into the free-streaming part, $\partial_t f+v\partial_x f=0$, and into the acceleration part, $\partial_t f-E\partial_v f=0$. Both parts are solved by integrating along the characteristics of the respective differential equation. Because of the periodic boundary conditions in x space, we interpolate the distribution function $f(*,v,t)$ using Fourier polynomials. In the v space, homogenous boundary conditions are used, and $f(x,*,t)$ is interpolated using splines. The appropiate electric field is computed by using the Nunerical Algorithms Group routine D01GAF [23]. We test the theory by comparing the computed hydrodynamic moments with those calculated by the Vlasov code. We use a Langmuir oscillation with the parameter set $\epsilon=0.157$, $\sigma_x=10$, and $\sigma_t=25$ for which we have already calculated ΔN (Fig. 2). Figure 15, on the other hand, shows the density perturbation in space-time as obtained by the Vlasov code. In comparing both results, we find good agreement. We now increase the amplitude of the wave to $\epsilon=1.57$. The theoretical result shown in Fig. 16 is qualitatively unchanged. The numerical (Vlasov) result is shown in Fig. 17. In both plots the width of the density depression is about $\Delta x\sim 40$, followed by the streamers. Because of the influence of the $O(E^3)$ terms, which were neglected in the theoretical analysis, there are some differences in the streamers. Next, we investigate the velocity moments. Figure 18 shows the analytical result, and Figure 19 shows the Vlasov result.

Clearly, in both plots the velocity is antisymmetric with respect to the center of the applied wave. We can understand this fact by referring to macroscopic theory: On the slow time scale, we get $\partial_t u = -\partial_x(E^2/2)$, which is Newton's first law. As the Gaussian profile is an even function in space, u has an uneven symmetry. The result of a kinetic microscopic calculation differs from the macroscopic picture in the appearance of the wake field pattern. The influence of the streamers becomes clearer when we look at the pressure moment (Figs. 20 and 21). The discrepancy between the analytical and the numerical calculations is more noticeable for the pressure than for the density. To understand this fact, we refer to Sec. III, where we found a stronger impact of the ponderomotive memory effect on the higher moments. Even at $k=0$, the higher moments differ in their wake-field pattern. Now, we turn to the self-consistent problem: in addition to the electric field of the applied wave, we consider the self-electric-field of the plasma due to charge separation. We note in Fig. 22 that the region occupied by the wake field extends over the course of time. Note that the fast oscillations have not yet averaged out. We also recognize that there is no density depression inside the plasma. The ponderomotive force effect is thus shielded out by the internal high frequency wake field which establishes because of charge separation. As known from Zakharov's model [24] the formation of a density depression requires the mobility of the ions, which we have not taken into account. The wake field, however, survives charge separation.

V. SUMMARY

We have investigated the wake field generation by the ponderomotive memory effect. In Sec. II, we presented the passive response of electrons on the slow time scale under the assumption that resonant particle effects are negligible or weak, and developed the underlying picture of ponderomotive effects. We saw that even if the perturbation is weak ($|E|^2 \ll 1$) and the unperturbed plasma is assumed to be thermal, the explicit time dependency of E forces us to treat the problem kinetically: $\partial_t|E|^2$ acts as a source and excites an infinite number of hydrodynamic moments almost spontaneously in the case of a short pulse. The main effect of $\partial_t|E|^2$, namely, the generation of wakes, can therefore not be found and studied rigorously within a macroscopic description of ponderomotive effects. In Sec. III, we investigated the problem in the absence of self-fields by using the method of characteristics. This treatment includes resonant particle effects. We then compared both methods by computing the hydrodynamic moments. We found that for small wave numbers ($k \leqslant 0.2$), neglecting resonant particle effects is justified. In Sec. IV, we used a Vlasov simulation to check these results. Perturbating a Maxwellian plasma with an electric field we found good agreement with our theoretical results in the non-self-consistent problem. However, in the self-consistent problem we obtained an unexpected result: the disappearence of the density depression. We explained this by the fact that, in the case of immobile ions, an internal high frequency field is generated by charge separation, and balances the ponderomotive force action of the applied high frequency wave packet.

ACKNOWLEDGMENTS

U.W. wishes to thank the Konrad-Adenauer-Stiftung for supporting this project. We are indebted to M. Glaser and F. Schmögner for their help in preparing the manuscript.

[1] T. Tajima and J. M. Dawson, Phys. Rev. Lett. **43**, 267 (1979).
[2] M. Y. Yu, P. K. Shukla, and N. L. Tsintsadze, Phys. Fluids **25**, 1049 (1982).
[3] P. Chen, J. M. Dawson, R. W. Huff, and T. Katsouleas, Phys. Rev. Lett. **54**, 693 (1985).
[4] R. Ruth, A. Chao, P. Morton, and P. Wilson, Part. Accel. **17**, 171 (1985).
[5] R. Keinigs and M. E. Jones, Phys. Fluids **30**, 252 (1985).
[6] P. Sprangle, E. Esarey, and A. Ting, Phys. Rev. Lett. **64**, 2011 (1990).
[7] F. F. Chen, in *Handbook of Plasma Physics*, edited by M. N. Rosenbluth and R. Z. Sagdeev, Physics of Laser Plasma Vol. 3 (Elsevier, Amsterdam, 1991), p. 483.
[8] P. Sprangle and E. Esarey, Phys. Fluids B **4**, 2241 (1992).
[9] G. Matthieussent, Phys. Scr. **T50**, 51 (1994).
[10] J. S. Wurtele, Phys. Today **47(7)**, 33 (1994).
[11] K. Nakajima *et al.*, Phys. Rev. Lett. **74**, 4428 (1995).
[12] A. Modena *et al.*, Nature (London) **377**, 606 (1995).
[13] Ch. J. Joshi and P. B. Corkum, Phys. Today **48(1)**, 36 (1995).
[14] D. L. Fisher, T. Tajima, M. C. Downer, and C. W. Siders, Phys. Rev. E **51**, 4860 (1995).
[15] C. V. Bulanov, T. Zh. Esirkepov, F. F. Kamenets, and N. M. Naumova, Sov. J. Plasma. Phys. **21**, 584 (1985) [Plasma Phys. Rep. **21**, 550 (1995)].
[16] H. Schamel and Ch. Sack, Phys. Fluids **23**, 1532 (1980).
[17] H. Schamel and Ch. Sack, in *Proceedings of the 2nd Joint Grenoble-Varenna International Symposium on ''Heating in Toroidal Plasma''* [ECSC-EEC-EAEC (Euratom), Brussels, 1981)], Vol. II, p. 1123.
[18] R. L. Stenzel and W. Gekelman, Phys. Fluids **20**, 108 (1977).
[19] V. B. Krapchev, Phys. Rev. Lett. **42**, 497 (1979).
[20] R. E. Aamodt and M. C. Vella, Phys. Rev. Lett. **39**, 1273 (1977).
[21] H. Schamel, Phys. Rev. Lett. **42**, 1339 (1979).
[22] C. Z. Cheng and G. Knorr, J. Comput. Phys. **22**, 330 (1976).
[23] The NAG Fortran Library Manual, The Numerical Algorithms Group Limited, 1988.
[24] V. E. Zakharov, Zh. Eksp. Teor. Fiz. **62**, 1745 (1972) [Sov. Phys. JETP **35**, 908 (1972)].